

# Investigation of Failure Mechanism of a DCI Engine Connecting Rod

Mustafa Guven Gok<sup>1,2,\*</sup> , Omer Cihan<sup>3,4</sup> 

<sup>1\*</sup> Department of Materials Science and Engineering, Hakkari University, Hakkari, Turkey. (m.guvengok@hakkari.edu.tr)

<sup>2</sup> Former Research Assistant at Department of Metallurgy and Materials Engineering, Istanbul Technical University, Istanbul, Turkey. (mngok@itu.edu.tr)

<sup>3</sup> Department of Mechanical Engineering, Hakkari University, Hakkari, Turkey. (omercihan@hakkari.edu.tr)

<sup>4</sup> Former Research Assistant at Department of Mechanical Engineering, Istanbul Technical University, Istanbul, Turkey. (ocihan@itu.edu.tr)

## ARTICLE INFO

Received: Jun., 24. 2021

Revised: Sep., 03. 2021

Accepted: Sep., 06. 2021

### Keywords:

Failure analysis

Connecting rod

Stress

Fatigue

Finite element analysis

Corresponding author: *Mustafa Guven*

*Gok*

ISSN: 2536-5010 / e-ISSN: 2536-5134

DOI: <https://doi.org/10.36222/ejt.957287>

## ABSTRACT

In reciprocating engines, connecting rod cap and connecting bolts are critical as they are exposed to varying loads under different operating conditions. This paper focuses on the failure of the connecting rod of a 1.5 dci K9K diesel engine. As a result of the engine operating for approximately 378400 km, the connecting rod was broken, and the reasons for the failure of the connecting rod cap and connecting bolt were investigated. The connecting rod of the K9K engine was designed in accordance with the dimensions by using SolidWorks software, and then exported to ANSYS software for stress and fatigue analysis. Also, the macrostructure of the broken connecting rod cap and bolt was investigated. We knew that the mechanic who fixed the engine about two years ago tightened the connecting rod bolts without using a torque meter. Therefore, stress and fatigue analyses were performed to determine the effect of different tightening torques (ranging from 22.5 to 52.5 Nm) at 2000 rpm. According to the numerical analysis results, with increasing tightening torque, the maximum equivalent stress and alternating stress values increased significantly, while the fatigue safety factor and the cyclic life of the connecting rod decreased. First, a fatigue fracture occurred in the right hand bolt. Immediately after, the lower cup deformed and crashed to the cylinder liner. Therefore, a brittle fracture occurred on the left shoulder of the connecting rod shank. The chevron markings were clearly visible in the macrostructure as evidence of brittle fracture.

## 1. INTRODUCTION

Connecting rods are critical among reciprocating engine parts. It provides the connection between the piston and the crankshaft. The thrust force generated on the piston surface is transmitted to the crank shaft through the connecting rod, and then work is obtained by the rotation of the crankshaft [1]–[3]. Therefore, it is exposed to compression load as a result of combustion and tensile load due to inertia. A connecting rod must withstand these high cyclic loads for a long time (usually at least  $10^8$  cycles) [4], [5]. As a result, analyzes such as stress, fatigue and failure detection in the connecting rod have become important.

In researches made to date, the study of the connecting rod failure analysis was carried out in many ways. Many factors such as fatigue and improper material selection, poor design or fabrication defects, overload bending, incorrectly adjusted bolts, application of excessive load to critical stress areas, coupling and assembly deficiencies lead to failure in the connecting rod part [6]–[8]. Most of the failures occur in some parts of the connecting rod, such as the rounded fillet of the big connecting rod end [9], over the connecting rod body [10],

the small head of the connecting rod, the crank pin, the roller bearing and the connecting rod bolt [11]. Rakic et al. [12] conducted a failure analysis of the connecting rod in a 12-cylinder diesel engine. Structural steel marked 18H2N4MA was used as connecting rod material. Besides chemical and metallographic analysis, the stress distribution under maximum load has been evaluated. The location of the fracture in the analysis is consistent with the highest stress zone obtained in the experiment. The fracture occurred at the length of the connecting rod close to the piston pin. Juarez et al. [13] discussed the results of a failure analysis study in the connecting rod of a diesel engine used in electrical power generation. AISI / SAE 4140 low alloy steel material is used in the connecting rod. According to the experimental and microstructural analysis of the study, the connecting rod has fractured in the body in a section close to the crankshaft side. The source of the fracture was determined in the crankshaft lubrication channel. The lubrication channel has been found to have been embedded in the surface, possibly as a result of an incomplete manufacturing process of tungsten-based material from a machining tool. The purpose of use of this material is that it is more suitable for the application area in

terms of chemical composition and mechanical properties. [13]–[15]. Rezvani et al. [16] studied the catastrophic deformation of the 645E3B engine connecting rod due to unknown reasons. The used connecting rod has 42CrMo4 material. Critical loads and buckling forces on the connecting rod were calculated using ADAMS software. It turns out that the connecting rod failure is due to buckling with the hydrolock phenomenon. Rabb [17] analyzed the fatigue failure of a connecting rod in a medium speed diesel engine. 34CrNiMo6TQ + T was used as the connecting rod material. It had been found to be failure near the crankshaft side. The screw thread profile has been changed to prevent failure, and the connecting rod material has been changed to increase fatigue strength. Bari et al. [18] conducted a finite element analysis simulation to determine the cause of the failure connecting rod from a motorcycle engine. Simulation in the ANSYS software was used to verify the surface failure and strength studied. The connecting rod material is AISI 4140 steel, and it has broken at the big end and the bolt housing of the connecting rod. It was concluded that the connecting rod failed at the end of the exhaust stroke due to the fatigue loading.

The connecting rod must be able to withstand enormous loads and transfer large amounts of power smoothly. According to Lee et al. [19], failure usually occurs at the big end of the connecting rod. The stress distribution was estimated and the value of the corner radius was optimized by using ANSYS software. Andoko et al. [20] investigated the cause of the failure of a connecting rod in a car. AISI 4315 material was used. As a result, big near-edge cracks had greater stress and strain values than the far area. Mirehei et al. [21] investigated the problem of the connecting rod fatigue failure of the universal tractor (U650) by using ANSYS software. This research demonstrated the occurrence of fatigue failure in the connecting rod due to continuous cyclic loads and variable speeds. Thomas et al. [22] indicated that the probability of fatigue failure due to fluctuation of loads was very high. Dupare et al. [22] stated that 50-90% of the failure in the connecting rod was due to fatigue failure. For this reason, authors were emphasized that it was very important to consider fatigue failure in connecting rod design. Ranjbarkohan et al. [23] performed an analysis of a Samand engine connecting rod for fatigue failure using the ANSYS workbench. Maximum tensile and compression load was applied to assess critical failure points to improve the strength and life of the connecting rod. According to the analysis results, the maximum tension (297.361 MPa) was determined at the pin end.

Another issue that needs to be considered is the stress and failure analysis of the connecting rod in diesel engines. Witek and Zelek [24] conducted a study on the failure and stress analysis of the connecting rod of a turbocharged diesel engine. ANSYS software was used for analysis. In the nonlinear static analysis results, it was determined that the high stress regions were located at the crack centers during the operation of the engine with maximum power. The results showed that the bolt tightening torque has a significant effect on the maximum stress value at the center of the crack. When the results of the study are examined, the main cause of the failure of the connecting rod was the high pretension of the bolts and the high stresses in the areas near the bolt hole. Griza et al. [25] examined the fatigue of the engine connecting rod bolt due to the laps occurring. The torque disassembly of the connecting rod bolts was monitored, and the fractured parts were

examined in the laboratory. A finite element analysis based on an analytical fracture mechanics approach was carried out to evaluate the relationship between tightening force and fatigue crack propagation in connecting rod bolts. It has been suggested that engine collapse was caused by the forming laps in the grooves of the bolt shank. Zhu et al. [26] made a failure analysis of the connecting rod cap and connecting bolts for a reciprocating compressor. The reasons for the failure of the connecting rod cap and connecting bolts as a result of operation for approximately 175.200 hours were researched. In the study, microstructure (by using scanning electron microscope (SEM) and optical microscope) and chemical composition of the connecting rod material were examined, and tensile, hardness and impact tests were applied. Moreover, the general stress distributions in the connecting rod were evaluated based on the maximum stress criterion using the finite element method. Looking at the results of the research, it was determined that the cause of the failure was high cycle fatigue, and the initial crack location was consistent with the high stress concentration. Acri et al. [27] scrutinized the coating processes of bolts and their effects on fatigue life of the connecting rod. As a result, it was thought that the stress concentration factor was smaller than the first engaged thread and the failure to the head was caused by thread rolling in the connecting rod.

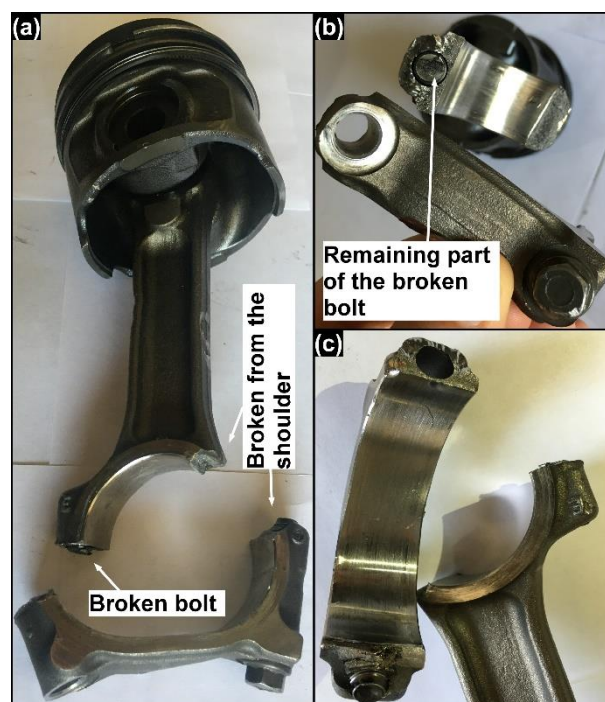


Figure 1. Macro view of the connecting rod after failure. (a) general view, (b) and (c) broken parts.

In this study, a broken connecting rod belonging to Renault Kangoo vehicle with 1.5 dci K9K (55kW) diesel engine was used. To simulate fatigue and stress distributions on the connecting rod, it was drawn according to its original dimensions by using SolidWorks software, and this drawn part was exported to ANSYS software. Different tightening torque values (22.5, 27.5, 32.5, 37.5, 42.5, 47.5 and 52.5 Nm),

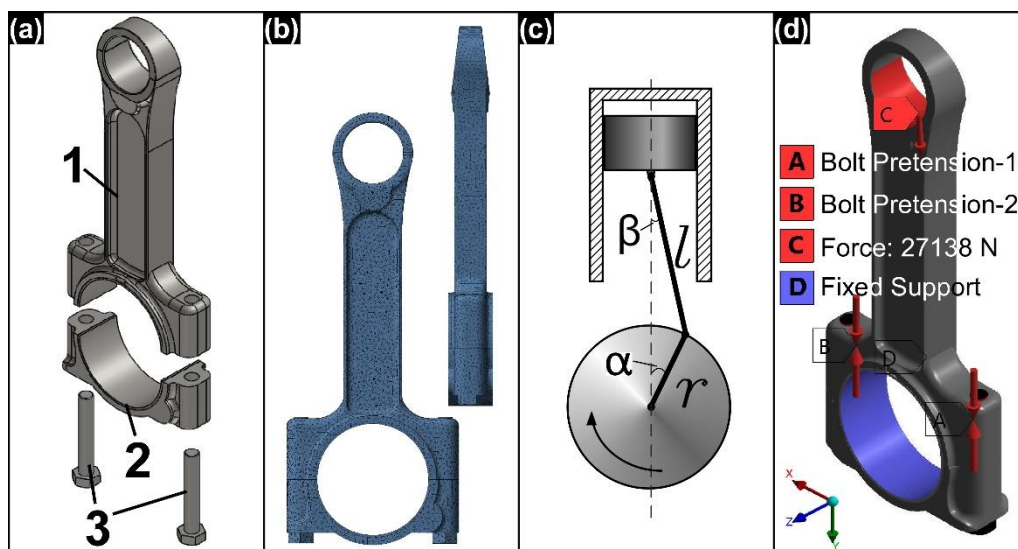


Figure 2. (a) Main parts of connecting rod, (b) finite element model showing meshes, (c) angles of crankshaft and connecting rod at the maximum in cylinder pressure, (d) loading conditions.

were evaluated at 2000 rpm. The fatigue behavior, maximum equivalent stress distributions, safety factor and alternating equivalent stress were analyzed to determine the effect of different tightening torques. Moreover, microstructural analysis was carried out to determine failure mechanism of the connecting rod.

## 2. MATERIALS AND METHOD (Helvetica 10p Bold)

### 2.1. Definition of failure and damaged connecting rod

The K9K type diesel engine used for power of a 2003 model Renault Kangoo type vehicle failed during operation. This engine had a turbocharger and a maximum power of 55 kW as can be seen from the detailed properties given in Table I.

TABLE I.  
PROPERTIES OF K9K ENGINE [28].

Number of cylinders	4
Bore	76 mm
Stroke	81 mm
Compression ratio	18.3
Rated power	55 kW / 3900 rpm
Maximum torque	156 Nm / 2000 rpm
Admission type	Turbocharged

When the engine was disassembled, one of the connecting rods was found to be broken. The vehicle was known to be at 378400 km when the failure occurred. Also, about 2 years ago from the connecting rod failure, the crankshaft was changed for another reason, and therefore the connecting rods were removed and reassembled. However, it was learned that the mechanic did not use a torque meter during this removal and reassembly of the connecting rods. The connecting rod was removed, and as seen in Figure 1 (a), in the big end region, the left bolt connecting the lower cap and the upper cup of the connecting rod was broken in the middle. The remaining part of bolt on the connecting rod shank could be seen in Figure 1 (b). The bolt on the right was intact (Figure 1 (a and c)). However, the right side of the connecting rod was broken from the big end shoulder. Also the lower cap of the big end was deformed.

### 2.2. Numerical model, meshing, boundary and loading conditions of the connecting rod

To understand the mechanism of connecting rod failure, first, the geometric model of the connecting rod was created using SolidWorks software. As seen in Figure 2 (a), the connecting rod consisted of three basic components. Part 1, 2 and 3 were the connecting rod shank, lower cap and bolts, respectively. Then, the created model was exported to the ANSYS Workbench software for numerical analysis. AISI 4140 low alloy steel was defined as the material with linear-elastic properties [13]. The maximum young's modulus, yield strength, ultimate strength and poisson ratio of 4140 steel were 210 GPa, 1540 MPa, 2073 MPa and 0.29 %, respectively. In the next step the contact definitions between neighboring components were carried out. The friction coefficients of bolts and all other parts were defined as 0.15 and 0.1  $\mu$ , respectively [24]. Tetrahedron meshes were used to divide the connecting rod into finite elements (Figure 2 (b)). The average mesh quality value was tried to be 0.85 and above to obtain more accurate results. To achieve this, different operations such as patch independent, patch conforming and mesh sizing were applied. The model was occurred with 160994 nodes and 104508 elements.

In this study, as mentioned above, failure analysis of connecting rod of K9K diesel engine was made. In order to calculate the maximum load acting on the connecting rod in this engine, the maximum in-cylinder pressure must first be determined. Nutu et al [28] reported that maximum in cylinder pressure of K9K engine was about 58 bar at 2000 rpm and 70% load. This value was converted to the newton force by using Equation 1. The angle of  $\alpha$  was 3.55 degrees, as the maximum pressure occurred when the crank angle was 10° after top dead center (ATDC) (see Figure 2 (c)) [29]. As seen in Figure 2(d), the load was applied according to this angular value. On the other hand, net force acting on connecting rod was calculated by using Equation 2. The force arising from inertia ( $F_{inertia}$ ) of the connecting rod and reciprocating mass, and force arising from friction ( $F_{friction}$ ) of the piston rings, and the piston were calculated according to Equations 3 and 4, respectively.

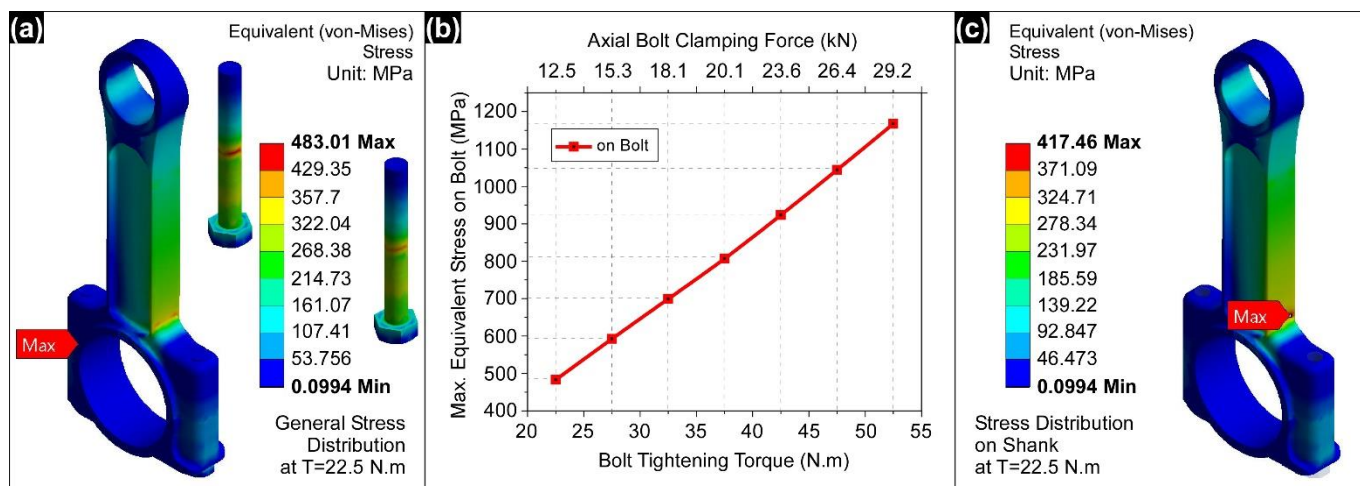


Figure 3. (a) equivalent (von-Mises) stress distributions on the all components of connecting rod, (b) graph of max. equivalent stress values on the bolt as a function of bolt tightening torque, (c) equivalent stress distributions on the connecting rod shank.

$$F_{gas} = \frac{\pi \cdot d^2}{4} * P_e \quad (1)$$

$$F = F_{gas} + F_{inertia} - F_{friction} \quad (2)$$

$$F_{inertia} = M * \omega^2 * r * (\cos\alpha + r * \frac{\cos\alpha}{l}) \quad (3)$$

$$F_{friction} = h * \pi * d * i * P_r * \mu \quad (4)$$

Here,  $M$  was mass of piston and rings + Piston pin + 1/3 rd of the connecting rod.  $\omega$ ,  $r$  and  $l$  were angular speed (rad/s), crank radius (mm) and length of the connecting rod (mm), respectively.  $\alpha$  was crank angle ( $^\circ$ ). Moreover, different bolt pressures were applied to the bolts as seen in Figure 2 (d). The required normal bolt tightening torque value was obtained from the K9K engine workshop repair manual (Renault Technical note) [30]. This value was  $20 \pm 2 \text{ Nm} + 45^\circ \pm 6^\circ$ , and it converted to the clamping force (N) value by using simply Equation 5.

$$T = K * F * d \quad (5)$$

Here,  $T$ ,  $K$  and  $F$  were tightening torque (Nm), a constant factor and the clamping force (N), respectively.  $d$  was the diameter (m) of the bolt. According to this formula, the clamping force at the normal tightening torque was about 12500 N. Big end bearing surfaces of the connecting rod was fixed as fixed support.

### 2.3. Analyzes

Six different (abnormal) tightening torque values, which are above the given normal value, were used to perform the numerical analysis of the failure of the connecting rod.

Because as mentioned above, during the previous engine repair, the mechanic tightened the connecting rod bolts without using a torque meter. The maximum equivalent stresses (von Mises) were analyzed to determine the effect of different tightening torques. In addition, fatigue analyzes were made in each case according to Goodman stress theory. The minimum life (cycles) and safety factor values were determined. During the analyses, the ambient temperature was set to  $95^\circ\text{C}$ .

## 3. RESULTS AND DISCUSSION

### 3.1. Stress Analysis

As a result of nonlinear static analyzes performed with the application of different bolt pretensions, maximum equivalent stress values in the connecting rods were obtained (Table II). During the analyses, bolt pre-tensions caused by different tightening torques varying in between 22.5 - 52.5 Nm were applied to the connecting rod. As seen in Figure 3 (a), the zone of maximum equivalent stress (483.01 MPa) at normal bolt tightening torque (22.5 Nm) was observed at the left-side bolt. This zone corresponded to the junction of the lower and upper cup of the connecting rod. In fact, as seen in Figure 1, the bolt on the left-side was broken at this zone. This equivalent stress value was considerably lower than the yield strength value of the bolt (1540 MPa). Therefore, at normal tightening torque, the stress safety factor in this zone was about "3.2" and it did not pose any problem. However, as seen in Figure 3 (b), the maximum stress value in this region significantly increased with the increase of the tightening torque. Such that, at the 52.5 Nm tightening torque, the maximum equivalent stress value on the bolt was 1167.5 MPa. This meant that the stress safety factor was approximately "1.3".

TABLE II.  
RESULTS OF STRESS AND FATIGUE ANALYSES.

Bolt tightening torque (Nm)	Axial bolt clamping force (N)	Force due to combustion (N)	Equivalent stress (N)	Equivalent alternating stress (N)	Safety factor for fatigue	Life (cycle) $\times 10^7$
22.5	12500	27138	483.01	284.72	1.9878	$1 \times 10^3$
27.5	15278	27138	592.35	359.53	1.6208	$1 \times 10^3$
32.5	18056	27138	699.23	437.05	1.3731	$1 \times 10^3$
37.5	20883	27138	806.89	519.96	1.1899	$1 \times 10^3$
42.5	23611	27138	923.52	615.78	1.0396	$3.45 \times 10^2$
47.5	26389	27138	1044.1	722.13	0.91952	6.81
52.5	29167	27138	1167.5	839.37	0.8224	$2.25 \times 10^{-1}$

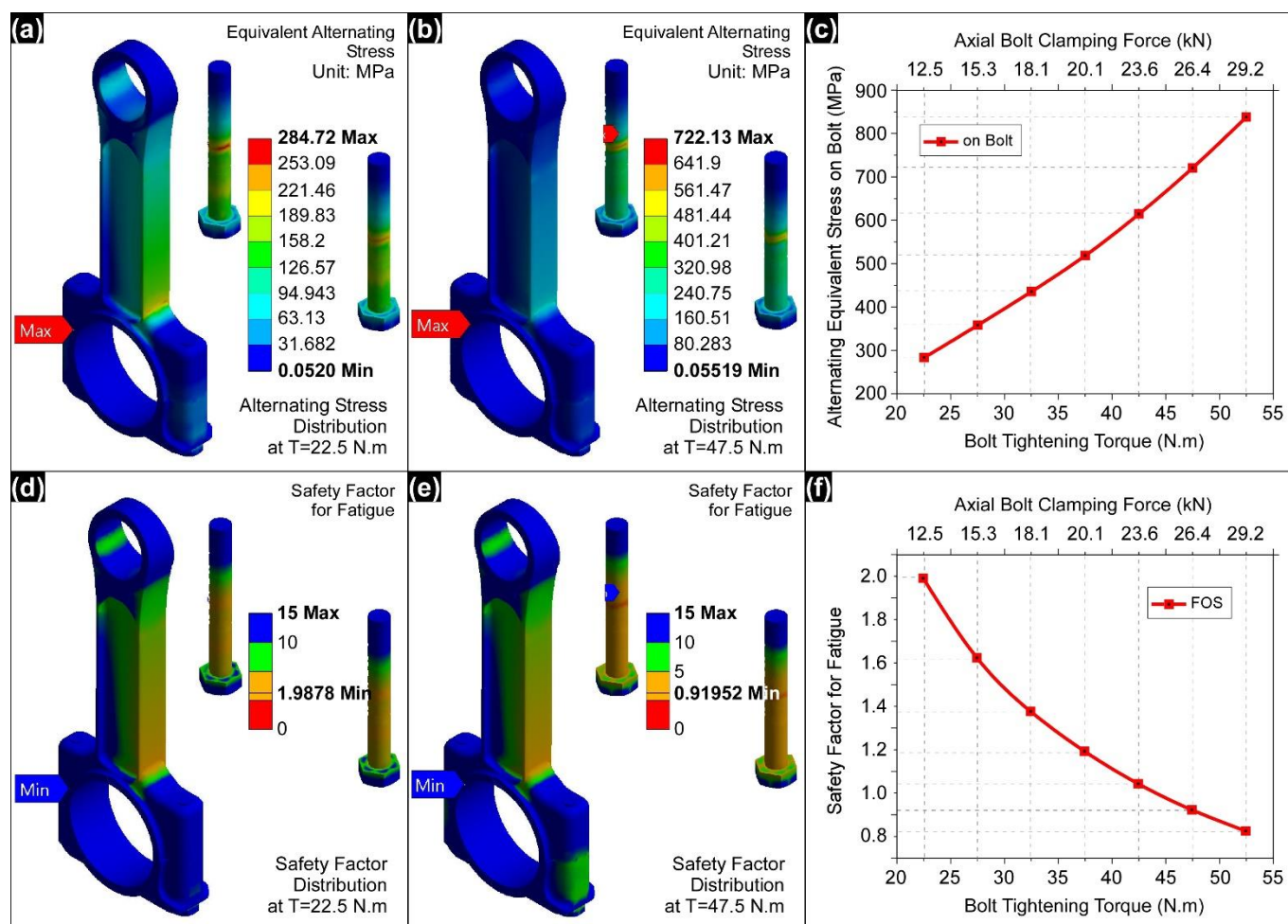


**Figure 4.** (a) Distribution of equivalent alternating stress at  $T=22.5$  Nm, (b) distribution of equivalent alternating stress at  $T=47.5$  Nm, (c) graph of alternating stress vs bolt tightening torque, (d) distribution of safety factor for fatigue at  $T=22.5$  Nm, (e) distribution of safety factor for fatigue at  $T=47.5$  Nm and (f) graph of safety factor for fatigue vs bolt tightening torque.

Witek et al. [24] stated that connecting rod bolts were subjected to complex loads acting as both tension and compression during engine operation. Therefore, the risk of breaking of the connecting rod bolts was high when the bolts were tightened above the normal tightening torque. On the other hand, as seen in Figure 3 (c), the maximum stresses on the connecting rod shank were concentrated in the right shoulder zone (417.46 MPa). This zone (right shoulder region of the connecting rod) was also the region where the break in the connecting rod shank occurred (see Figure 1). Because the maximum in cylinder pressure occurred when the crank angle was  $10^\circ$  after the piston top dead center, the load was applied to the piston pin of the connecting rod at an angle of  $3.55$  degrees. Therefore, the zones where the stresses concentrated on the components of connecting rod and the zones where the fractures occurred were completely matched.

### 3.2. Fatigue Analysis

Fatigue analyzes were performed on the model to determine the effect of non-normal bolt tightening torque on the life of connecting rod components. During engine operation, connecting rods are subjected to cycling compression due to combustion force and tensile load due to inertia of moving parts [31]. Therefore, these loads should be considered in order to obtain realistic results in numerical modeling. As mentioned above, the maximum compression force due to combustion was 27138 N, and the tensile force due to inertia of moving parts was 1243 N. Hence, the ratio of

-0.046 was used for the stress-life fatigue analysis. As expected, equivalent alternating stresses were concentrated on the bolt where equivalent stresses were maximum (see Figure 1 (a and b)). The maximum value of equivalent alternating stress considerably increased with increasing bolt tightening torque. While the maximum value of equivalent alternative stress was 284.72 MPa at normal bolt tightening torque (22.5 Nm), this value increased to 839.37 MPa at 52.5 Nm bolt tightening torque (Figure 1 (a-c)). Tabulated data including all the results of the fatigue analysis are given in Table II. Tabulated data including all the results of the fatigue analysis were given in Table II. On the other hand, as seen in Figure 4 (d-f), safety factor values for fatigue decreased with the increasing bolt tightening torque. At normal bolt tightening torque, safety factor for fatigue was about "1.99" (Figure 4 (d and f)). This value was quite satisfactory in terms of fatigue. However, this value was lower than "1", especially with the application of 47.5 Nm and higher bolt tightening torque (Figure 4 (e and f)). This greatly increases the likelihood of fatigue damage. As Consistent with this, as seen in Table II, at 42.5, 47.5 and 52.5 Nm bolt tightening torque values, the fatigue life of connecting rod decreased to  $3.45 \times 10^9$ ,  $6.81 \times 10^7$  and  $2.25 \times 10^6$  cycles, respectively. As explained in the previous section, the zones where alternating stresses and minimum safety factors

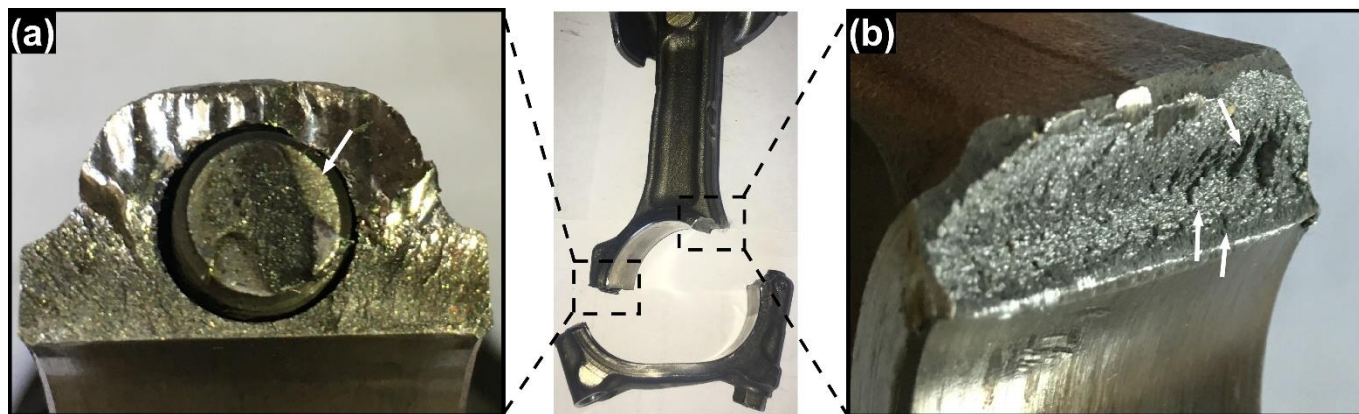


**Figure 5.** Macrostructure of damaged zones. (a) fracture surface of the remaining part of the broken left side bolt and (b) fracture surface of the broken right side shoulder.

concentrated were the points where breakage occurred in the connecting rod (left bolt and right shoulder).

### 3.3. Macrostructural investigation and failure mechanism

The macrostructural photograph of the damaged zones of the connecting rod was given in Figure 5 (a and b). In Figure 5 (a), the possible fatigue area in the remaining part of the broken bolt is indicated by the arrow. Due to the fact that the mechanic did not use a torque meter, fatigue occurred in the over-tightened bolt, and the remaining section of the bolt after the fatigue damage area was broken because it could not bear the axial clamping force. As proved in the previous sections, the stresses in the broken region of the bolt were maximum and the safety factors were minimum. Immediately after the bolt on the left broke, the right shoulder area of the connecting rod was overloaded (stresses were also concentrated in this area as the maximum cylinder pressure took place at the crank angle of  $10^\circ$  ATDC). The deformed lower cap hit the cylinder liner and broke on the right shoulder and completely separated from the connecting rod shank. As a result, a brittle fracture occurred in the right shoulder region (Figure 5 (b)). As evidence of this, chevron markings (indicated by arrows in Figure 5 (b)) were observed in the fracture zone. Because it was reported that chevron markings typically result from the brittle fracture of steel materials [32]. Then the rings and valves took damage due to the uncontrolled movement of the piston. Thus, the connecting rod bolt, which had fatigue fracture due to excessive tightening torque, caused the connecting rod to break completely and the engine to be seriously damaged.

## 4. CONCLUSIONS

The present work was aimed to determine failure mechanism of a K9K diesel engine connecting rod. Existing connecting rod was broken from right side bolt and left side shoulder (on shank). We knew that the mechanic who fixed the engine about two years ago tightened the connecting rod bolts without using a torque meter. Therefore, stress and fatigue analyzes were performed to determine the effect of different tightening torques (ranging from 22.5 to 52.5 Nm) at 2000 rpm. The maximum equivalent stress and alternating stress values increased from 483.01 to 1167.5 MPa and 284.72 to 839.37 MPa, respectively. After a tightening torque of 42.5 Nm, the fatigue safety factor was lower than "1", and cycling life decreased up to  $2.25 \times 10^6$  cycles. The points where the failure in the connecting rod occurred and the zones where the stresses concentrated in the analyzes were compatible. Firstly, a fatigue

fracture occurred in the right hand bolt. Immediately after, the lower cup deformed and crashed to the cylinder liner. Therefore, a brittle fracture occurred on the left shoulder of the connecting rod shank. The chevron markings were clearly visible in the macrostructure as evidence of brittle fracture. As a result, the use of torque meters was very important in the assembly of engine post-repair parts.

## ACKNOWLEDGEMENT

The authors would like to thank Istanbul Technical University Information Technologies Directorate for permission the use of the softwares.

## REFERENCES

- [1] S. Fukuda and H. Eto, 'Development of fracture splitting connecting rod', *JSAE Rev.*, vol. 23, no. 1, pp. 101–104, 2002, doi: 10.1016/S0389-4304(01)00154-0.
- [2] Z. Pan and Y. Zhang, 'Numerical investigation into high cycle fatigue of aero kerosene piston engine connecting rod', *Eng. Fail. Anal.*, vol. 120, pp. 1–13, 2021, doi: 10.1016/j.engfailanal.2020.105028.
- [3] A. Gautam, 'Static Stress Analysis of Connecting Rod Using Finite Element Approach', *IOSR J. Mech. Civ. Eng.*, vol. 10, no. 1, pp. 47–51, 2013, doi: 10.9790/1684-1014751.
- [4] P. Singh, D. Pramanik, and R. V. Singh, 'Fatigue and Structural Analysis of Connecting Rod's Material Due to (C.I) Using FEA', *Int. J. Automot. Eng. Technol.*, vol. 4, no. 4, pp. 245–253, 2015.
- [5] A. Muhammad, M. A. H. Ali, and I. H. Shanono, 'Design optimization of a diesel connecting rod', *Mater. Today Proc.*, vol. 22, pp. 1600–1609, 2019, doi: 10.1016/j.matpr.2020.02.122.
- [6] B. yan He, G. da Shi, J. bing Sun, S. zhuan Chen, and R. Nie, 'Crack analysis on the toothed mating surfaces of a diesel engine connecting rod', *Eng. Fail. Anal.*, vol. 34, pp. 443–450, 2013, doi: 10.1016/j.engfailanal.2013.09.004.
- [7] X. L. Xu and Z. W. Yu, 'Failure analysis of a diesel engine connecting rod', *J. Fail. Anal. Prev.*, vol. 7, no. 5, pp. 316–320, 2007, doi: 10.1007/s11668-007-9058-9.
- [8] G. T. Reddy and C. Srinivas, 'Fatigue analysis and life predictions of Forged steel and Powder Metal connecting rods', *IOSR J. Mech. Civ. Eng.*, vol. 16, no. 053, pp. 15–19, 2016, doi: 10.9790/1684-16053031519.
- [9] M. N. Ilman and R. A. Barizy, 'Failure analysis and fatigue performance evaluation of a failed connecting rod of reciprocating air compressor', *Eng. Fail. Anal.*, vol. 56, pp. 142–149, 2015, doi: 10.1016/j.engfailanal.2015.03.010.
- [10] M. N. Mohammed, M. Z. Omar, S. Zainuddin, A. Salah, M. A. Abdelgnei, and M. S. Salleh, 'Failure analysis of a fractured connecting rod', *J. Asian Sci. Res.*, vol. 2, no. 11, pp. 737–741, 2009.
- [11] S. Khare, O. P. Singh, K. Bapanna Dora, and C. Sasun, 'Spalling investigation of connecting rod', *Eng. Fail. Anal.*, vol. 19, no. 1, pp. 77–86, 2012, doi: 10.1016/j.engfailanal.2011.09.007.
- [12] S. Rakic, U. Bugaric, I. Radisavljevic, and Z. Bulatovic, 'Failure analysis of a special vehicle engine connecting rod', *Eng. Fail. Anal.*, vol. 79, no. April, pp. 98–109, 2017, doi: 10.1016/j.engfailanal.2017.04.014.

- [13] C. Juarez, F. Rumiche, A. Rozas, J. Cuisano, and P. Lean, 'Failure analysis of a diesel generator connecting rod', *Case Stud. Eng. Fail. Anal.*, vol. 7, pp. 24–31, 2016, doi: 10.1016/j.csefa.2016.06.001.
- [14] A. Saravanan, P. Suresh, G. Sudharsan, and V. Suresh, 'Static analysis and weight reduction of aluminum casting alloy connecting rod using finite element method', *Int. J. Mech. Prod. Eng. Res. Dev.*, vol. 8, no. 3, pp. 507–518, 2018, doi: 10.24247/ijmperdjun201855.
- [15] P. Sarate, G. R. Kesheorey, and M. Shah, 'A Comparative Study on Forecasting and Analysis of 4140 Material Composition of Connecting Rod for Various Applications', no. November, 2017.
- [16] M. A. Rezvani, D. Javanmardi, and P. Mostaghim, 'Diagnosis of EMD645 diesel engine connection rod failure through modal testing and finite element modeling', *Eng. Fail. Anal.*, vol. 92, no. January, pp. 50–60, 2018, doi: 10.1016/j.engfailanal.2018.05.005.
- [17] R. Rabb, 'Fatigue failure of a connecting rod', *Eur. Struct. Integr. Soc.*, vol. 22, no. C, pp. 97–112, 1997, doi: 10.1016/S1566-1369(97)80011-8.
- [18] K. Bari, A. Rolfe, A. Christofi, C. Mazzuca, and K. V. Sudhakar, 'Forensic investigation of a failed connecting rod from a motorcycle engine', *Case Stud. Eng. Fail. Anal.*, vol. 9, no. May, pp. 9–16, 2017, doi: 10.1016/j.csefa.2017.05.002.
- [19] S. Y. Lee, S. B. Lee, H. S. Kim, T. G. Kim, M. G. Kam, and J. W. Yoon, 'Failure Analysis of Connecting Rod at Big End', *Key Eng. Mater.*, vol. 306–308, pp. 345–350, 2006, doi: 10.4028/www.scientific.net/kem.306-308.345.
- [20] A. Andoko *et al.*, 'Failure analysis on the connecting rod by finite element method', *AIP Conf. Proc.*, vol. 2262, no. September, 2020, doi: 10.1063/5.0015728.
- [21] A. Mirehei, M. Hedayati Zadeh, A. Jafari, and M. Omid, 'Fatigue analysis of connecting rod of universal tractor through finite element method (ANSYS)', *J. Agric. Technol.*, vol. 4, no. 2, pp. 21–27, 2008.
- [22] T. G. Thomas, S. Srikari, and M. L. Suman, 'Design of Connecting Rod For Heavy Duty Applications Produced By Different Processes For Enhanced Fatigue Life', *SasTech J.*, vol. 10, no. 1, pp. 1–7, 2011.
- [23] M. Ranjbarkohan, M. R. Asadi, M. Mohammadi, and A. Heidar, 'Fatigue analysis of connecting rod of samand engine by Finite Element Method', *Aust. J. Basic Appl. Sci.*, vol. 5, no. 11, pp. 841–845, 2011.
- [24] L. Witek and P. Zelek, 'Stress and failure analysis of the connecting rod of diesel engine', *Eng. Fail. Anal.*, vol. 97, pp. 374–382, 2019, doi: 10.1016/j.engfailanal.2019.01.004.
- [25] S. Griza, F. Bertoni, G. Zanon, A. Reguly, and T. R. Strohaecker, 'Fatigue in engine connecting rod bolt due to forming laps', *Eng. Fail. Anal.*, vol. 16, no. 5, pp. 1542–1548, 2009, doi: 10.1016/j.engfailanal.2008.10.002.
- [26] X. Zhu, J. Xu, Y. Liu, B. Cen, X. Lu, and Z. Zeng, 'Failure analysis of a failed connecting rod cap and connecting bolts of a reciprocating compressor', *Eng. Fail. Anal.*, vol. 74, pp. 218–227, 2017, doi: 10.1016/j.engfailanal.2017.01.016.
- [27] A. Acri, S. Beretta, F. Bolzoni, C. Colombo, and L. M. Vergani, 'Influence of manufacturing process on fatigue resistance of high strength steel bolts for connecting rods', *Eng. Fail. Anal.*, vol. 109, no. May 2019, p. 104330, 2020, doi: 10.1016/j.engfailanal.2019.104330.
- [28] N. C. Nutu, C. Pana, N. Negurescu, A. Cernat, D. Fuioreescu, and L. Nemoianu, 'An experimental approach on fuelling a passenger car diesel engine with LPG', *IOP Conf. Ser. Mater. Sci. Eng.*, vol. 444, no. 7, 2018, doi: 10.1088/1757-899X/444/7/072001.
- [29] M. Tuti, Z. Şahin, and O. Durgun, 'Thermodynamic diesel engine cycle modeling and prediction of engine performance parameters', *Gmo-Shipmar*, vol. 207, no. March, pp. 14–26, 2017, [Online]. Available: [https://www.journalagent.com/gmo/pdfs/GMO\\_23\\_207\\_14\\_26.pdf](https://www.journalagent.com/gmo/pdfs/GMO_23_207_14_26.pdf).
- [30] Renault, 'Technical Note6006A KXX, and K9K engine - Engine workshop repair manual', 2004.
- [31] M. T. Alam, A. Thakur, V. Kumar PS, and S. Ghadei, 'Fatigue Failure Analysis of Diesel Engine Connecting Rod', in *SAE Technical Papers*, Jul. 2018, vol. 2018-July, pp. 1–8, doi: 10.4271/2018-28-0067.
- [32] J. W. Sowards, C. N. McCowan, and E. S. Drexler, 'Interpretation and significance of reverse chevron-shaped markings on fracture surfaces of API X100 pipeline steels', *Mater. Sci. Eng. A*, vol. 551, pp. 140–148, 2012, doi: <https://doi.org/10.1016/j.msea.2012.04.108>.

## BIOGRAPHIES

**Mustafa Guven Gok** graduated from Firat University department of Metallurgical Education with a bachelor and master of science degrees in 2008 and 2010, respectively. After, he graduated from Istanbul Technical University department of Metallurgical and Materials Engineering in 2015 with Ph.D. degree. Dr. Gok joined to the Materials Science and Engineering Department of Hakkari University in 2015 and he has been working in Hakkari University since 2016. His study fields include: Plasma Spray Coating and Spark Plasma Sintering (SPS) Processes, Thermal Barrier Coatings, Self-Healing Ceramics, Biomaterials, Finite Element Analysis and Materials of Internal Combustion Engine.

**Omer Cihan** born in 1986, studied Mechanical Training. He completed his MSc degrees in department of Mechanical Training from Firat University, Elazığ, Turkey, in 2011. Then, He completed his PhD degrees in Mechanical Engineering from Istanbul Technical University, Istanbul, Turkey, in 2017. He has been worked as a research assistant at University of Istanbul Technical, Mechanical Engineering Department, Turkey, from 2010 to 2017. He is currently working at Hakkari University, Turkey, as Assist. Professor. The primary topics of his scientific work are such as Engine materials, Friction, Wear, Engine testing, Engine performance and emissions, Engine construction, Rotary engine, Engine electronic control unit and Internal combustion engine.